Inertial Ferrofluidic Sensor for Vibration, Displacement and Impulse Measurement with a Linear Output Signal

Koskov M.A., Somov S.A., Krylasova O.S., Ivanov A.S.
"Institute of Continuous Media Mechanics of the Ural Branch of the Russian Academy of Sciences" is a branch of the Federal State Budgetary Scientific Institution Perm Federal Research Center of the Ural Branch of the Russian Academy of Sciences
Perm, Russian Federation

Abstract. The aim of the work is to develop the uniaxial ferrofluid sensor suitable for use either as an accelerometer for low-frequency vibrations or as a ballistic device or seismic sensor for shock loads. The goal is achieved by solving the following problems: development of a magnetic suspension system with a linear axial gradient of the magnetic field strength, calculation of the viscous friction force of the magnetic fluid filling the coaxial layer between the magnetic cylinder and the non-magnetic body wall, manufacturing of the sensor and its static and dynamic tests. The most significant result of the work is the experimental confirmation of the linearity of the electromechanical system of the sensor, corresponding to the model representations of a linear dissipative oscillating system with one degree of freedom. The significance of the obtained results lies in the appearance of cheap and simple linear inertial sensors. The principle of operation of the sensor is based on the registration of the motion of an inert mass deviating from the equilibrium position under the action of an external force to be measured. The inert mass, consisting of ring permanent magnets, levitates in a coaxial layer of magneto-fluid lubricant. The sensor, depending on its parameters, can measure either quasi-static force, or force impulse, or coordinate displacement, which is in demand in monitoring systems for critical structures and buildings, as well as in navigation systems for vehicles operating under conditions of small, slowly changing accelerations (microgravity).
Keywords: magnetic fluid, inertial sensor, permanent magnet, viscous friction.

DOI: https://doi.org/10.52254/1857-0070.2024.4-64.07
UDC: 53.084

Senzor ferrofluid inerțial pentru măsurarea vibrațiilor, deplasării și impulsurilor de forță cu semnal de ieșire linear

Koskov M.A., Somov S.A., Krâlasova O.S., Ivanov A.S.
„Institutul de Mecanică Continuă a Filialei Ural a Academiei Ruse de Științe” - o ramură a Instituției Federale de Științe Bugetare de Stat a Centrului Federal de Cercetare Perm al Filialei Ural a Academiei Ruse de Științe,
Perm, Federatia Rusă
Rezumat. Scopul lucrării este de a dezvolta un senzor ferofluid uniaxial adecvat pentru a fi utilizat fie ca accelerometru pentru vibrații de joasă frecvență, fie ca dispozitiv balistic sau senzor seismic pentru încărcări de șoc. Obiectivul este atins prin rezolvarea următoarelor probleme: dezvoltarea unui sistem de suspensie magnetică cu un gradient axial liniar al intensității câmpului magnetic; calcularea forței de frecare vâscoasă a fluidului magnetic care umple stratul coaxial dintre cilindrul magnetic și peretele corpului nemagnetic; fabricarea senzorului și testele sale statice și dinamice. Cel mai semnificativ rezultat al lucrării este confirmarea experimentală a liniarității sistemului electromecanic al senzorului, care corespunde reprezentărilor modelului unui sistem oscilant disipativ liniar cu un grad de libertate. Semnificația rezultatelor obținute constă în apariția unor senzori inerțiali liniari ieftini și simpli. Principiul de funcționare al senzorului se bazează pe înregistrarea mișcării unei mase inerte care se abate de la poziția de echilibru sub acțiunea unei forțe externe care trebuie măsurată. Masa inertă, formată din magneți permanenți inelari, levitează într-un strat coaxial de lubrifiant magneto-fluid. Senzorul, în funcție de parametrii săi, poate măsura fie forța cvasi-statică, fie impulsul forței, fie deplasarea coordonatelor, care este solicitată în sistemele de monitorizare pentru structuri și clădiri critice, precum și în sistemele de navigație pentru vehicule care funcționează în condiții de accelerații mici, care se modifică lent (microgravitație).
Cuvinte-cheie: fluid magnetic, senzor inerțial, magnet permanent, frecare vâscoasă.

Инерционный магнитожидкостный датчик для измерения вибраций, смещений и импульса силы с линейным выходным сигналом

Косков М.А., Сомов С.А., Крыласова О.С., Иванов А.С.

«Институт механики сплошных сред Уральского отделения Российской академии наук» - филиал Федерального государственного бюджетного учреждения науки Пермского федерального исследовательского центра Уральского отделения РАН, Пермь, Российская Федерация

Аннотация. Целью работы является разработка одноосного инерционного магнитожидкостного регистрирующего прибора (датчика), пригодного к использованию либо в качестве акселерометра при низкочастотных вибрациях, либо баллистического прибора или сейсмодатчика при ударных нагрузках. Поставленная цель достигается за счёт решения следующих задач: разработка системы магнитного подвеса с линейным осевым градиентом напряжённости магнитного поля; расчёт силы вязкого трения магнитной жидкости, заполняющей коаксиальный слой между магнитным цилиндром и немагнитной стенкой корпуса; изготовление датчика и проведение его статических и динамических испытаний на вибростенде. Наиболее существенным результатом работы является экспериментальное подтверждение линейности электромеханической системы датчика, соответствующей модельным представлениям о линейной диссипативной колебательной системе с одной степенью свободы, что позволяет описывать работу датчика неоднородным линейным дифференциальным уравнением второго порядка. Значимость полученных результатов заключается в появлении дешёвых и технологически простых в изготовлении линейных инерционных магнитожидкостных датчиков, способных измерять ударные и низкочастотные механические нагрузки. Принцип работы датчика основан на регистрации движения инертной массы, отклоняющейся от положения равновесия под действием внешней силы, подлежащей измерению. Измерительная подсистема датчика реализована в виде оптической схемы, что исключает её взаимодействие с телом и с системой магнитного подвеса посредством магнитного поля (распространённый недостаток ранних конструкций). Датчик обладает цилиндрической симметрией. Инертная масса, состоящая из кольцевых постоянных магнитов, левитирует в коаксиальном слое магнитожидкостной смазки. Датчик, в зависимости от его параметров, может измерять или квазистатическую силу (акселерометр), или импульс силы (баллистический датчик), или смещение по координате (сейсмодатчик), что востребовано в системах мониторинга ответственных конструкций и зданий, а также в системах навигации аппаратов, функционирующих в условиях малых, медленно меняющихся ускорений (микрогравитация).

Ключевые слова. магнитная жидкость, инерционный датчик, постоянный магнит, вязкое трение.

INTRODUCTION

Mechanical sensors, such as quasi-static recorders of low frequency forces, force pulses, and seismic sensors [1], are widely used in industry, construction [2, 3], including power complex facilities, aircraft [4], etc. Alternative microelectromechanical (MEMS), piezoelectric, and fiber optic sensors are also popular due to their small size and weight [5]. However, their production requires complex and proprietary microelectronics manufacturing technologies, leading to high financial costs.

In contrast, inertial mechanical sensors are larger and heavier but structurally simpler and more affordable than integrated circuits. An inertial sensor's core component is an inert mass - a body resting on an elastic suspension that responds to the action of external forces. The use of magnetic fluid (MF) [6, 7] has enabled both a simpler sensor design and higher sensitivity to small accelerations (approximately $10^{-4}\,g$) [8]. This sensitivity is at least one order of magnitude higher than comparable characteristics (approximately $10^{-2} - 10^{-3}\,g$) of commercially available devices, such as those manufactured by Analog Devices using iMEMS technology. MF is a stable colloidal solution of ferri- or ferromagnetic particles in a nonmagnetic carrier fluid, making it suitable for use in the design of supports, bearings, dampers, measuring devices, and seals [9, 10]. An inert mass made of permanent magnets floats in this colloid in a suspended state [11], without contacting the walls of the sensor body (levitating). Here, the MF acts as a lubricant, replacing dry friction with liquid friction, which increases the sensitivity of the measuring device.

The use of a MF suspension makes it possible to create inertial sensors with a specific design, first patented in the 1970s [8] and subsequently developed further in the 1990s [3, 12 − 15] and into the XXI century [16 − 25]. In the uniaxial design [14, 18 − 25], the sensor body is a hollow, non-magnetic tube housing an inert mass, with the entire structure exhibiting cylindrical symmetry. The gap between the inert mass and the body is filled with a MF droplet. The displacement $z(t)$ of the mass from its equilibrium position z_0 over time t is described by the equation of forced oscillations [1]

$$\frac{d^2 z}{dt^2}+2\gamma\frac{dz}{dt}+\omega_0^2 z=f(t) \qquad (1)$$

where $f(t)$ – is the external force normalized to the mass of the sensing element – the signal to be measured. The sensor's useful signal is generated by measuring $z(t)$, and the unknown force f is calculated using the coefficients γ and ω_0 which are sensor parameters. The frequency of natural oscillations of the inert mass ω_0 is determined by the balance of inertial and return forces in the absence of external influence and friction (dissipation) forces.

In sensor designs [14, 18, 21 − 25], the return force arises from the repulsion of the magnetic sensing element [22 − 25] by a system of permanent magnets and/or coils placed on the device body. The coefficient γ represents the viscous friction occurring in the layer of MF. The inertial force is determined by the mass of the body, which can be adjusted by using composite constructions of magnetic and nonmagnetic materials with different densities.

The combined effect of inertial, frictional, and return forces completely and uniquely determines the sensor type [1]. In quasi-static devices (constant force recorders), inertial and friction forces are minimal in comparison to the return force

$$\left|\mathrm{d}^2 z/\mathrm{d}t^2\right| \ll \left|\omega_0^2 z\right|,$$
$$\left|2\gamma\left(\mathrm{d}z/\mathrm{d}t\right)\right| \ll \left|\omega_0^2 z\right|.$$

A seismic device (displacement recorder) is characterized by four conditions: small friction and return forces compared to the inertia force

$$\left|2\gamma\left(\mathrm{d}z/\mathrm{d}t\right)\right| \ll \left|\mathrm{d}^2 z/\mathrm{d}t^2\right|,$$
$$\left|\omega_0^2 z\right| \ll \left|\mathrm{d}^2 z/\mathrm{d}t^2\right|,$$

as well as high quality factor and significant frequency deviation (the minimum frequency in the signal spectrum $f(t)$ should exceed ω_0). For a ballistic device (force pulse sensor), the parameters must meet two conditions. The first condition imposes a restriction on the sensor's natural oscillation period: it must be significantly larger than the characteristic time τ of the measured impact $2\pi/(\omega_0^2-\gamma^2)^{0.5} \gg \tau$. The second condition requires high Q-factor of the oscillating system, $Q=\omega_0/(2\gamma) \gg 1$.

Regardless of the sensor's purpose, the coefficients ω_0 and γ must remain constant to enable an unambiguous interpretation of $f(t)$ based on the signal magnitude $z(t)$. This condition is fulfilled only for linear oscillating systems, for which the principle of superposition of signals is true, and their functioning is described by a system of linear algebraic or integro-differential equations [1].

Previously, we proposed a method for designing sensors that satisfy the requirement ω_0 = const [26] and investigated the viscous friction of a coaxial magnetic fluid layer in the gap between a magnetic inertial mass and a nonmagnetic tube, simulating the device body [27]. The present work is devoted to the experimental verification of model (1) as applied to a laboratory prototype of a uniaxial inertial sensor we developed [28], using both static and dynamic tests.

I. MATERIALS AND METHODS

The laboratory mockup of an inertial MF sensor suitable for dynamic testing was constructed from independent modules. The first module was an axisymmetric magnetic suspension system designed to return the inertial mass to the geometric center of the device. The system [26], based on two axially magnetized ring permanent magnets and a coil with a rectangular cross-section, was used as the general concept. Barium ferrite magnets with a residual magnetization of 300 kA/m were utilized. The coil was designed for low heat dissipation (< 3 W) at a current density of 1 A/mm². The final configuration of the magnetic system is shown in fig. 1. The magnetic field along its axis has a linear gradient (fig. 2), with $H \propto z^2$, a $\nabla H \propto z$. This results in a linear return force $m\omega_0^2 z$ exerted by the magnetic suspension on the inertial mass m. The magnetic system was mounted on a 3D-printed plastic housing, providing a large safety margin and high resistance to deformation (fig. 3).

An assembly of five NdFeB ring permanent magnets, separated by plastic inserts, was used as the inertial mass (fig. 4). This combination of alternating magnets and non-magnetic washers serves two purposes. First, it enables adjustment of the body's average density. Second, the alternating magnetic rings create a magnetic field (fig. 5) that provides a high bearing capacity of approximately ~ 10 N/cm² for the MF layer [29], ensuring near-complete coaxial alignment of the inertial mass within the cylindrical channel, regardless of the sensor's spatial orientation.

Experimental tests [27] and numerical simulations using FEMM (finite element method magnetics) software confirmed that this design allows the MF to fully occupy the coaxial gap between the assembly and the tube (fig. 5). Partially filling the gap with individual MF droplets [23 − 25] results in a strong, unpredictable dependence of the friction coefficient γ on the sensing element's velocity, which is unsuitable for sensors. The mass of the sensing element without MF was 1.59 g.

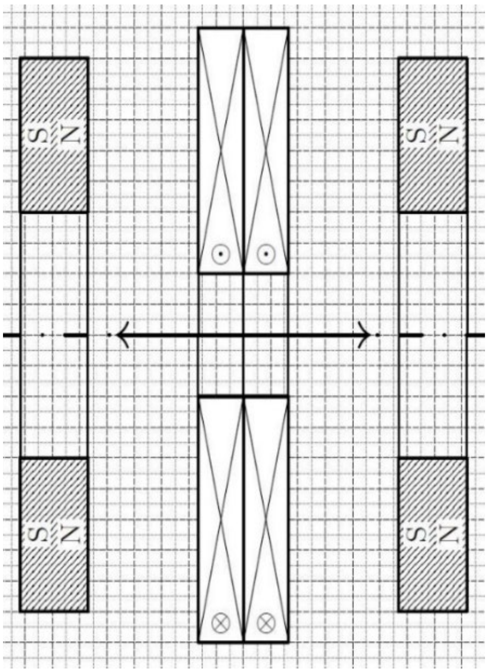

Two-pointed arrow denotes the linearity area, background cell scale is 2 mm.

Fig. 1. Configuration of the magnetic system with a linear axial gradient of the magnetic field strength.

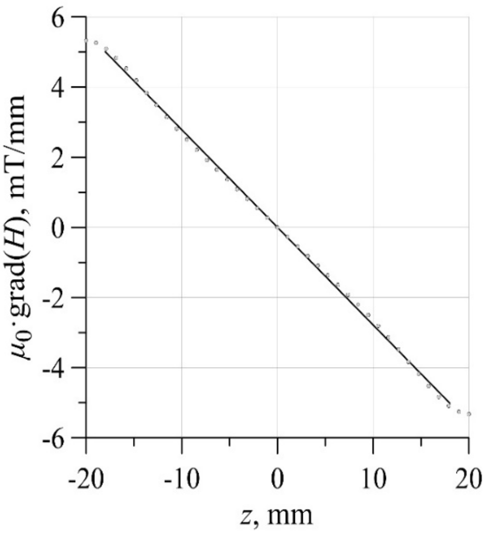

Dots refer to calculation, straight line shows the linear approximation, μ_0 – universal magnetic constant.

Fig. 2. Calculated gradient of the field strength along the axis of the magnetic system.

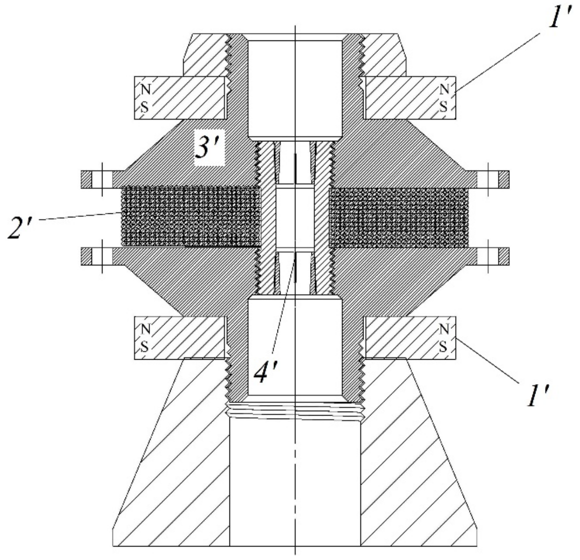

Ring magnet 1', coil 2', plastic housing 3', sensing element location 4'.

Fig. 3. Axial section of the inertial ferrofluid sensor demonstrating it construction and components layout.

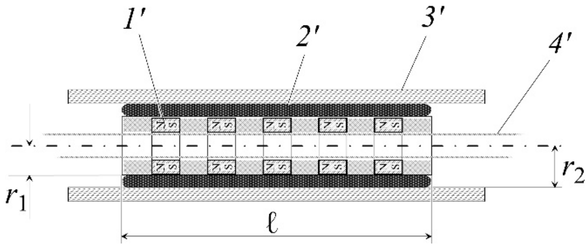

Permanent magnets 1', MF 2', sensor housing 3', non-magnetic rods 4'

Fig. 4. Schematic of the sensing element.

The linearity of the return force $m\omega_0^2 z$ was verified by measuring it as a function of displacement z from the equilibrium position z_0. For this measurement, the sensing element's stem (fig. 4) was securely attached to a dynamometer.

Fig. 6 shows the force as a function of the sensing element's displacement from the sensor's center. The angular coefficient of the fitted line $m\omega_0^2$ = 19.2 mN/mm was measured with an error of less than 2 %, yielding an estimated natural frequency of ω_0 = 110 rad/s.

Considering the mass of the MF ≈ 0.07 g filling the gap between the element and the housing, the adjusted estimate for the circular frequency is 107 rad/s.

The maximum value of the friction coefficient γ was estimated using the formula [27]

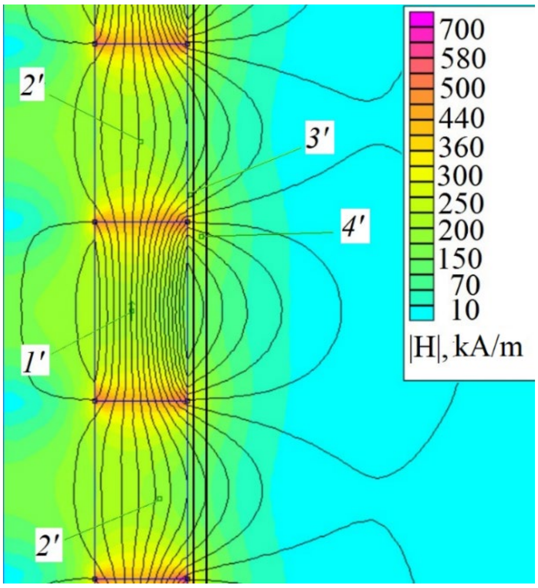

Permanent ring magnets 1′, plastic inserts 2′, epoxy resin coating 3′, gap between the sensing element and the sensor body filled with magnetic fluid 4′.

Fig. 5. Magnetic field strength modulus generated by the sensing element.

$$\frac{\gamma m}{\eta \ell} = \frac{\pi}{\ln R_2} + \pi\left[\frac{2R_2^2}{R_2^2-1} - \frac{1}{\ln R_2}\right] \times \frac{2R_2^2 \ln R_2 - R_2^2 + 1}{\left(R_2^2+1\right)\ln R_2 - R_2^2 + 1} \qquad (2)$$

Here $R_2 = r_2 / r_1$ is the ratio of the inner radius of the tube $r_2 = 2.21$ mm to the outer radius of the sensing element $r_1 = 2.07$ mm, $\ell = 22.0$ mm (see fig. 4), $\eta_0 = 13.6\cdot10^{-3}$ Pa·s is the viscosity of the MF measured by a rotational viscometer at room temperature. A theoretical estimation of the friction coefficient $\gamma \approx 30$ s^{-1}. Following the sensor classification given earlier, we calculate the period $2\pi/(\omega_0^2-\gamma^2)^{0.5} \approx 0.06$ s, and the quality factor $Q = \omega_0/(2\gamma) \approx 2$. These estimations mean that the made mockup is a ballistic device for measuring a force pulse with a characteristic exposure time on the order of 1 ms. At the same time $Q \approx 2$ means low sensitivity of the mockup and a significant contribution of viscous dissipative forces to the formation of a useful signal. In future prototypes of the sensor, of course, the value of the friction coefficient will be reduced by at least an order of magnitude by increasing the parameter R_2 and using a less viscous carrier fluid (PES-1).

For further reasoning and estimation, let us assume that oscillations in the investigated system (1) take the form $z(t) \propto \cos(\omega t)$. Thus, $|d^2z/dt^2| = \omega^2 z$, and $|2\gamma(dz/dt)| = 2\gamma\omega z$. Consequently, the setup will function as a quasi-static force recorder when the conditions $\omega^2 \ll \omega_0^2$ and $2\gamma\omega \ll \omega_0^2$ are met. The first condition implies that the frequency of external forcing $\omega < 30$ rad/s, and the second condition gives an estimate of $\omega < 20$ rad/s. Here and below, the symbol "$\ll$" is used to mean "10 times less" – a standard approach for numerical estimation in vibration theory and radio engineering [30]. The smallest of these estimates is preferred.

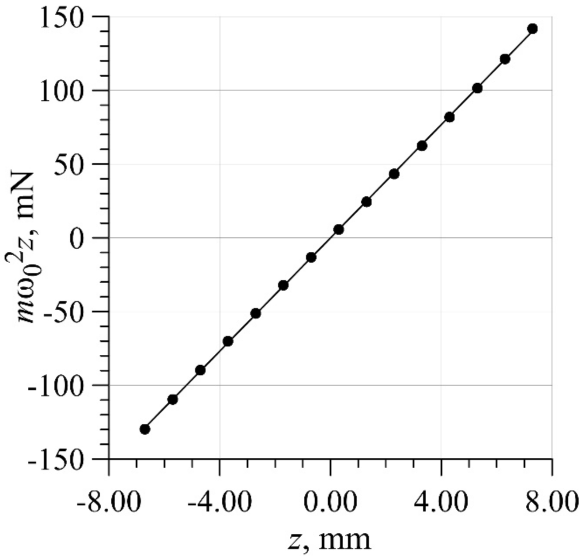

Dots - experiment, solid line – linear approximation.

Fig. 6. Force acting on the sensing element from the side of the magnetic system (Fig. 1).

It should also be noted that this model is not suitable as a seismic device (displacement meter) since a seismic device requires both a high quality factor $Q \gg 1$ and high inertia – conditions that are not met in this case. Thus, the model can operate as a quasi-static force recorder at characteristic frequencies of external influence in the range of 0 to 3 Hz, where the useful signal $z(t)$ is proportional to the magnitude of the external force $f(t)$.

In addition to static tests (fig. 6), dynamic tests of the assembled model were performed on a vibration test bench across a frequency range typical for mechanical vibrations, from 5 to 50 Hz (10π to 100π rad/s). A harmonic vibration of fixed amplitude and fixed frequency (constant during measurement) was used as the external force. The vibration was provided by a Brüel & Kjær 4828 modal exciter with an external automated control system "Visom". The control system feedback was achieved using a piezoelectric vibration accelerometer PCB352A25 mounted on the bench table. The setup is illustrated in fig. 7.

The tested model was positioned on the vibration table (*1′*), and the displacement amplitude A of the table was held constant across various vibration frequencies ω. The position $z(t)$ of the inert mass was measured with a Riftek-602 triangulation laser caliper (*2′*), which was focused on a reflective element (*3′*) attached to the inert mass's rod. This setup effectively prevented any direct influence of the MF on the $z(t)$ signal, representing a key innovation in our design. Unlike earlier designs (dating back to the 1970s), our sensor's measurement subsystem is entirely independent of the magnetic suspension system supporting the inert mass. This approach avoids unwanted inductive coupling between the device's modules and mitigates the adverse effect of magnetophoresis in the MF [31] on the $z(t)$ signal. Notably, magnetophoresis, manifesting as a time-dependent drift of the sensor's "zero" position $z_0 = z_0(t)$, has been a major obstacle to the large-scale production and broad adoption of such devices. In our design, the negative effects of magnetophoresis are largely eliminated.

Installing the caliper on a fixed mount (not shown in fig. 7) made it possible to protect the measuring system from vibration and, consequently, to improve the accuracy of measurements.

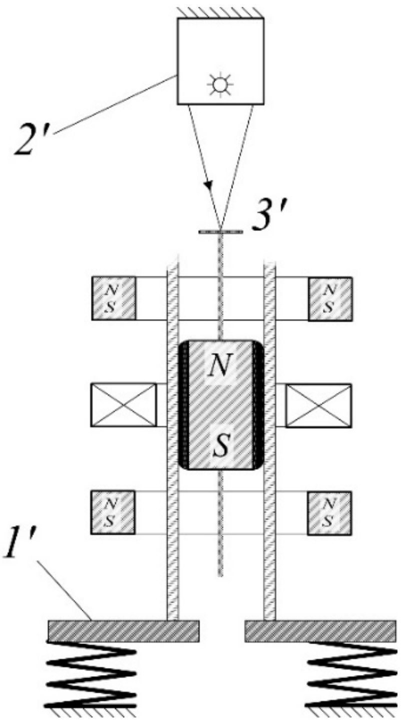

Modal exciter 1′, laser triangular caliper 2′, reflective element 3′ attached to the rod of the inertial mass.

Fig. 7. Schematic diagram of the experimental setup for vibration tests.

In such a formulation of the experiment equation (1) takes the form

$$\frac{d^2z}{dt^2} + 2\gamma\frac{dz}{dt} + \omega_0^2 z = \omega_0^2 Z + 2\gamma\frac{dZ}{dt} \qquad (3)$$

where z is the displacement of the inert mass relative to the stationary rangefinder, $Z = A\cdot\sin(\omega t)$ is a vertical displacement of the shaker table. The right part of the equation is the elastic and friction forces, respectively, acting from the side of the oscillating body of the layout on the sensitive element. In (3) the constant force of gravity g is not taken into account, which leads only to the change of the position of the origin of displacements z_0. The search for the steady-state solution of equation (3) in the form $z = a\cdot\sin(\omega t - \varphi)$ gives the vibration amplitude transfer coefficient

$$\frac{a}{A} = K(\omega) = \sqrt{1 - \frac{\omega^4 - 2\omega_0^2\omega^2}{\left(\omega^2 - \omega_0^2\right)^2 + 4\gamma^2\omega^2}} \qquad (4)$$

The application of this formula in analyzing the results of experiments explains the fixation of the amplitude of displacements A, instead of the often used amplitude of accelerations $\omega^2 A$.

II. RESULTS

In two test series, the steady-state vibration amplitudes of the sensitive element, a, were measured across different frequencies. These values were normalized by the table's vibration amplitude A, resulting in the amplitude-frequency characteristics $K(\omega)$ of the system under study (fig. 8). Due to the minimum sensitivity limits of the modal exciter's control system, which could not register vibration accelerations below 0.1 g, the tests were conducted at A = 0.5 mm starting from 7 Hz (44 rad/s) and at A = 1 mm from 5 Hz (31 rad/s). The experimental $K(\omega)$ values were fitted to formula (4) using the least squares method. As seen in fig. 8, there is excellent agreement between the experimental measurements and the fitted curves, with a slight exception around ω = 200 rad/s, which we attribute to minor inconsistencies in the modal exciter's operation at these frequencies. From the approximations, the resonance frequencies ω_r of the dissipative oscillating system (with one degree of freedom) were determined, and the results are presented in Table 1, along with the percentage deviations from their calculated values.

Table 1
Inertial magnetic fluid sensor properties obtained in dynamic tests

A, mm	ω_r, rad/s	$(\omega_r/\omega_0 - 1)$, %
0.50	116	5.5
1.00	114	3.5

As shown, the natural frequency of the inertial MF sensor obtained in dynamic tests is less than 10 % above the theoretical estimate and shows minimal dependence on the oscillation amplitude. Doubling the amplitude and quadrupling the corresponding oscillation energy do not lead to significant changes in ω_r. This confirms that the tested sensor model aligns closely with theoretical predictions for a linear oscillating system with one degree of freedom.

The linearity of the sensor is further supported by the static test results of the magnetic suspension (fig. 6), which demonstrate the linearity of the return force. Dynamic tests fully confirmed this linearity. This linear behavior enables the sensor to measure both static and dynamic forces of arbitrary shape accurately. In linear systems, the absence of combinational effects (such as the generation of harmonics at multiples of frequencies not present in the original signal) [32] and the applicability of the signal superposition principle ensure a clear, unambiguous correspondence between sensor readings and external influences of various spectra (within the device's technical specifications and intended application).

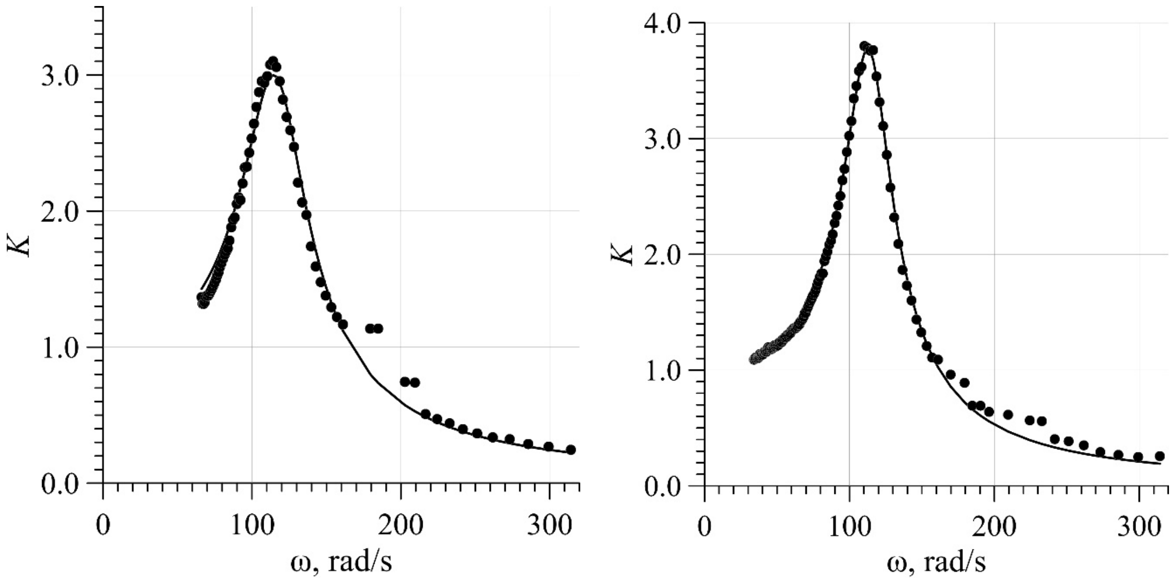

a) Amplitude is 0.5 mm, *b) amplitude is 1 mm,*
Dots - experiment, solid line - approximation by formula (4).
Fig. 8. Transmission coefficient of sinusoidal vibration amplitude as a function of ω.

Let us discuss an important question regarding the influence of temperature T and magnetophoresis of colloidal particles on sensor performance. In equation (1) T affects only the frictional force. Typically, the viscosity of liquids $\eta(T)$ decreases exponentially with increasing T, so $\gamma(T)$ also varies widely; however, this is not a problem. The device design should be based on the minimum operating temperature T_{min} specified for the sensor's intended climate range [33].

According to the earlier classification of sensors, the primary requirement for friction is that it remains small relative to the return force $\gamma \ll \omega_0$ and the inertia force, a requirement similar to the high quality factor condition $Q \gg 1$. If the inequality $\gamma(T_{min}) \ll \omega_0$ is met, the sensor will maintain its specified characteristics at any T.

The required value of $\gamma(T_{min})$ can be achieved either by adjusting parameter R_2 in (2) or by selecting a MF with low-viscosity carrier liquid with a suitable stabilizer [34].

Another phenomenon that negatively affects the performance of MF devices, especially sealers [35], is magnetophoresis [36 – 38], which results in spatial inhomogeneity of particle concentration ϕ and viscosity $\eta(T, \phi)$. The problem of flow in an inhomogeneous MF is simplified if the concentration and viscosity gradients ($\nabla\phi$ and $\nabla\eta$, respectively) have a single, non-zero radial component. This condition is satisfied if ∇H has a similar configuration. Although ∇H deviates from ideal linear dependence (see fig. 5), the magnetic assembly acts as a MF support, causing the colloid to distribute over its surface as a continuous, relatively uniform layer. The free surface of the MF satisfies H = const, approximating the cylindrical surface of the assembly. Consequently, in the first approximation, surfaces of equal concentration ϕ are also cylindrical. Additionally, equilibrium isolines of concentration near a permanent magnet are predominantly located along its surfaces [39, 40], further supporting $\nabla\eta = \{d\eta / dr; 0; 0\}$ in this context. The MF flow in a thin coaxial gap is planar [27], with the velocity vector $\mathbf{v} = \{0; \upsilon_z; 0\}$ orthogonal to $\nabla\eta$, so the flow does not alter ϕ. The viscous friction force $\propto \eta(r)(d\upsilon_z / dr)$ thus remains constant throughout the flow. Therefore, in the first approximation, magnetophoresis can be neglected in its effect on the friction coefficient γ.

III. Conclusions

The problems of designing, fabricating, and dynamically testing a uniaxial inertial sensor for mechanical actions, which includes a MF suspension for the sensing element (inert mass), have been addressed. An axisymmetric system has been fabricated that meets the requirements for linearity of the return force and low power consumption in inertial sensors. The sensor utilizes a sensing element, which is an assembly of magnetic and non-magnetic rings capable of maintaining continuous filling of the coaxial gap between the device's body and the inert mass with MF, thereby ensuring low friction. Theoretical estimates of the viscous friction coefficient and the natural frequency of the sensor were performed. The results of the dynamic tests align with the theoretical estimates. It is concluded that the sensor design fully corresponds to the model representations of a linear oscillating system with one degree of freedom. The significance of the obtained results lies in the potential for designing and manufacturing inexpensive and technologically simple linear inertial MF sensors, capable of measuring shock and low-frequency mechanical vibrations. This capability is beneficial for monitoring buildings and critical structures with sources of noise and vibration, such as hydraulic units in hydroelectric power plants [41].

Acknowledgement

The work was supported by Russian Science Foundation (Project No. № 23-21-00100).

References

[1] Bendrikov G.A., Ivanov I.V., Karasev M.D., Medvedev V.I., Minakova I.I., Senatorov K.Yu. *Teoriya kolebanij* [Theory of oscillations]. Moscow, 1983. 328 p.

[2] Hou R., Xia Y. Review on the new development of vibration-based damage identification for civil engineering structures: 2010–2019. *Journal of Sound and Vibration*, 2021, vol. 491, art.no. 115741. doi: 10.1016/j.jsv.2020.115741

[3] Pallarés F.J., Betti M., Bartoli G., Pallarés L. Structural health monitoring (SHM) and Nondestructive testing (NDT) of slender masonry structures: A practical review. *Construction and Building Materials*, 2021, vol. 297, art.no. 123768. doi: 10.1016/j.conbuildmat.2021.123768

[4] Popa N.C., Sabata I.De., Anton I., Potencz I., Vékás L. Magnetic fluids in aerodynamic measuring devices. *Journal of Magnetism and Magnetic Materials*, 1999, vol. 201, iss. 1 - 3, pp. 385 - 390. doi: 10.1016/S0304-8853(99)00148-1

[5] Mishra M.K., Dubey V., Mishra P.M., Khan I. Mems Technology: A Review. *Journal of Engineering Research and Reports*, 2019, vol. 4, no. 1, art.no. 46001.
doi: 10.9734/JERR/2019/v4i116891

[6] Rosensweig R. *Ferrohydrodynamics*. Cambridge, 1985.

[7] Bibik E.E., Lavrov I.S. *Sposob polucheniya ferrozhidkosti* [Method for producing ferrofluid]. Patent USSR, no. 457666, 1975.

[8] Bailey R.L. Lesser known application of ferrofluids. *Journal of Magnetism and Magnetic Materials*, 1983, vol. 39, iss. 1-2, pp. 178-182. doi: 10.1016/0304-8853(83)90428-6

[9] Zhang X., Sun L., Yu Y., Zhao Y. Flexible Ferrofluids: Design and Applications. *Advanced Materials*, 2019, vol. 31, art.no. 1903497. doi: 10.3390/mi10110744

[10] Nesterov S.A., Baklanov V.D. Development of a model and experimental study of thermal processes in a ferrofluid sealer. *Problemele Energeticii Regionale*, 2023, vol. 58, iss. 2. doi: 0.52254/1857-0070.2023.2-58-05

[11] Rosensweig R. Buoyancy and stable levitation of a magnetic body immersed in a magnetizable fluid. *Nature*, 1966, vol. 210, pp. 613-614. doi: 10.1038/210613a0

[12] Takaharu I., Ikuo H., Toshihisa I., Tatsuo S., Hideo I. Acceleration sensor. Patent EP, no. 0293784 B1, 1994.

[13] Tanaka S. Acceleration sensor. Patent JP, no. H08334529A, 1995.

[14] Raj K., Ionescu C. Ferrofluid inclinometer. Patent USA 5452520A, 1995.

[15] Piso M.I. Applications of magnetic fluids for inertial sensors. *Journal of Magnetism and Magnetic Materials*, 1999, vol. 201, pp. 380-384. doi: 10.1016/S0304-8853(99)00164-X

[16] Baglio S., Barrera P., Savalli N. Novel ferrofluidic inertial sensors. *IEEE Instrumentation and Measurement Technology Conference Proceedings*, Sorrento, 2006, pp. 2368-2372. doi: 10.1109/IMTC.2006.328622

[17] Simonenko D.V., Suprin A.E., Romanov Yu.I. Magnetofluidic accelerometer with active suspension. Patent USA, no. 0059990A1, 2006.

[18] Pristup A.G. Magnetofluidic unidirectional accelerometer. Patent USA, no. 0214889A1, 2007.

[19] Quan L., Li D. Use of Magnetic Fluid in Accelerometers. *Journal of Sensors*, 2014, vol. 2014, p. 9. doi: 10.1155/2014/375623

[20] Yao J., Li D. Research on the linearity of a magnetic fluid micro-pressure sensor. *Sensors and Actuators A: Physical*, 2015, vol. 229, pp. 36-41. doi: 10.1016/j.sna.2014.11.026.

[21] Saikin M.S., Morozova D.Yu. *Magnitozhidkostnoe ustrojstvo dlya opredeleniya ugla naklona* [Magneto-fluid tilt detection device]. Patent RU, no. 166054, 2016.

[22] Su S., Li D., Tan N., Li G. The study of a novel tilt sensor using magnetic fluid and its detection mechanism. *IEEE Sensors Journal*, 2017, vol. 17, no. 15, pp. 4708-4715. doi: 10.1109/JSEN.2017.2714689

[23] Lagutkina D.Yu, Saikin M.S. The research and development of inclination angle magnetic fluid detector with a movable sensing element based on permanent magnets. *Journal of Magnetism and Magnetic Materials*, 2017, vol. 431, pp. 149-151. doi: 10.1016/j.jmmm.2016.11.040

[24] Lagitkina D.Yu., Saikin, M.S. *Magnitozhidkostnoe ustrojstvo dlya opredeleniya ugla naklona* [Magneto-fluid tilt detection device]. Patent RU, no. 167814, 2017.

[25] Öztürk Y., Yariçi I. Research on a novel magnetic tilt sensor designed using Hall elements and ferrofluid. *Journal of Electrical Engineering*, 2019, vol. 70, iss. 5, pp. 406-411. doi: 10.2478/jee-2019-0073

[26] Koskov M.A., Ivanov A.S. *Magnitnaya sistema odnoosnogo inercionnogo magnitozhidkostnogo akselerometra* [Magnetic System of Uniaxial Ferrofluid Accelerometer]. *Vestnik IGEU*, 2022, no. 6, pp. 26-36. (In Russian) doi: 10.17588/2072-2672.2022.6.027-037

[27] Ivanov A.S., Koskov M.A., Somov S.A. Viscous friction of a ferrofluid in the coaxial gap between cylindrical walls in uniform rectilinear relative motion. *Bulletin of the Russian Academy of Sciences: Physics*, 2024, vol. 88, no. 7, pp. 1158-1165. doi: 10.1134/S1062873824707256.

[28] Ivanov A.S., Koskov M.A. *Magnitozhidkostnoe ustrojstvo dlya izmereniya linejnyh uskorenij i ugla naklona* [Magnetic fluid device for measuring linear accelerations and tilt angle]. Patent RU, no. 2788591, 2023.

[29] Bashtovoi V.G., Bossis G., Kabachnikov D.N., Krakov M.S., Volkova O. Modelling of magnetic fluid support. *Journal of Magnetism and Magnetic Materials*, 2002, vol. 252, pp. 315-317. doi: 10.1016/S0304-8853(02)00597-8

[30] Horowitz P., Hill W. *The art of electronics*. Cambridge, 2015.

[31] Polunin V.M., Ryapolov P.A., Bashtovoy V.G., Postnikov E.B., Shabanova I.A., Sokolov E.A., Zubkova E.A Magnetophoresis of microparticles in a magnetic fluid. *Russian Physical Journal*, 2021, vol. 64, pp. 478–486. doi: 10.1007/s11182-021-02352-z

[32] Zernov N.V., Karpov V.G. *Teoriya radiotekhnicheskih cepej* [Theory of radio engineering circuits]. Moscow-Leningrad, 1965. 892 p.

[33] *GOST 15150-69. Ispolneniya dlya razlichnyh klimaticheskih rajonov. Kategorii, usloviya ekspluatacii, hraneniya i transportirovaniya v chasti vozdejstviya klimaticheskih faktorov vneshnej sredy* [State Standard 15150-69. Machines, instruments and other industrial products. Modifications for different climatic regions. Categories, operating, storage and transportation conditions as to environment climatic aspects influence]. Moscow, Standartinform Publ., 2006, 57 p.

[34] Lebedev A.V., Lysenko S.N. Magnetic fluids stabilized by polypropylene glycol. *Journal of Magnetism and Magnetic Materials*, 2011, vol. 323, iss. 10, pp. 1198-1202. doi: 10.1016/j.jmmm.2010.11.005

[35] Sharyna S.G., Krakov M.S. Effect of a high-gradient magnetic field on particle concentration distribution in a magnetic fluid seal: rivalry of the diffusion and magnetophoresis. *Journal of Magnetism and Magnetic Materials*, 2024, vol. 599, art.no. 172095. doi: 10.1016/j.jmmm.2024.172095

[36] Bashtovoi V., Reks A., Kuzhir P., Zubarev A., Volkova O., et. al. Effect of magnetophoresis and Brownian diffusion on mechanical processes in magnetic fluids: the role of a condensation phase transition. *Journal of Magnetism and Magnetic Materials*, 2020, vol. 498, art.no. 166148. doi: 10.1016/j.jmmm.2019.166148.

[37] Bashtovoi V.G., Kuzhir P.P., Zubarev A.Yu., Moroz V.S. On the mechanics of magnetic fluids with field-induced phase transition: application to Couette flow. Magnetohydrodunamics, 2018, vol. 54, iss. 3, pp. 181-196. doi: 10.22364/mhd.54.3.1.

[38] Shi Z., Sun J., Jia S., Zhang P. Simulation of magnetophoresis of magnetic nanoparticles in liquids. *Journal of Physics D: Applied Physics*, 2016, vol. 49, art.no. 335005. doi: 10.1088/0022-3727/49/33/335005.

[39] Pshenichnikov A.F., Burkova E.N. Forces acting on a permanent magnet placed in a rectangular cavity with a magnetic fluid. *Computational Continuum Mechanics*, 2014, vol. 7, iss. 1, pp. 5-14. doi: 10.7242/1999-6691/2014.7.1.1

[40] Pshenichnikov A.F., Burkova E.N. Effect of demagnetizing fields on particle spatial distribution in magnetic fluids. *Magnetohydrodynamics*, 2012, vol. 48, no. 3, pp. 243-253. doi: 10.22364/mhd

[41] GuoW., Wu F. Hydraulic-mechanical coupling vibration performance of pumped storage power station with two turbine units sharing one tunnel. *Journal of Energy Storage*, 2022, vol. 53, art.no. 105082. doi: 10.1016/j.est.2022.105082

Information about the authors.

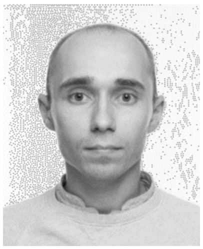

Koskov Mikhail Andreevich
Junior researcher at the Institute of Continuous Media Mechanics, Ural Branch of the Russian Academy of Sciences, Perm, Russia. Research interests: fluid mechanics.
E-mail: koskov.m@icmm.ru

Krylasova Olga Sergeyevna
Engineer at the Institute of Continuous Media Mechanics, Ural Branch of the Russian Academy of Sciences, Perm, Russia. Research interests: fluid mechanics.
E-mail: krylasova.o@icmm.ru

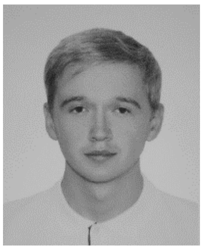

Somov Sergey Andreyevich
Engineer at the Institute of Continuous Media Mechanics, Ural Branch of the Russian Academy of Sciences, Perm, Russia. Research interests: fluid mechanics.
E-mail: somov.s@icmm.ru

Ivanov Aleksey Sergeyevich
Head of laboratory Dynamics of dispersed systems at the Institute of Continuous Media Mechanics, Ural Branch of the Russian Academy of Sciences, Perm, Russia. Research interests: fluid mechanics, magnetic measurements.
E-mail: lesnichiy@icmm.ru